Shift Factor-Based SCOPF Topology Control MIP Formulations with Substation Configurations

Evgeniy A. Goldis, Pablo A. Ruiz, *Member, IEEE,* Michael C. Caramanis, *Senior Member, IEEE,* Xiaoguang Li, C. Russ Philbrick, *Senior Member, IEEE,* Aleksandr M. Rudkevich, *Member, IEEE.*

Abstract—Topology control (TC) is an effective tool for managing congestion, contingency events and overload control. The majority of TC research has focused on line and transformer switching. Substation reconfiguration is an additional TC action, which consists of opening or closing breakers not in series with lines or transformers. Some reconfiguration actions can be simpler to implement than branch opening, seen as a less invasive action. This paper introduces two formulations that incorporate substation reconfiguration with branch opening in a unified TC framework. The first method starts from a topology with all candidate breakers open, and breaker closing is emulated and optimized using virtual transactions. The second method takes the opposite approach, starting from a fully closed topology and optimizing breaker openings. We provide a theoretical framework for both methods and formulate security-constrained shift factor MIP TC formulations that incorporate both breaker and branch switching. By maintaining the shift factor formulation we take advantage of its compactness, especially in the context of contingency constraints, and by focusing on reconfiguring substations we hope to provide system operators additional flexibility in their TC decision processes. Simulation results on a subarea of PJM illustrate the application of the two formulations to realistic systems.

I. Nomenclature

Vectors are indicated by lower case bold, matrices by upper case bold, and scalars by lower case italic characters indexed appropriately. Upper limits are indicated by an over-bar, and lower limits by an under-bar. Sensitivities are indicated with Greek characters. When a single set identifier is used as a superscript for a vector or matrix, we refer to the row elements of that vector or matrix corresponding to elements in the set. When two set identifiers are used as superscripts for a PTDF sensitivity matrix, the first applies to its rows and the second to its columns.

Sets

$\mathcal{Z}$ Set of candidate breakers (zero-impedance)
$\mathcal{N}$ Set of branches (non-zero impedance)
$\mathcal{M}$ Set of monitored branches

$\mathcal{S}$ Set of switchable branches
$\mathcal{R}$ Set of cutsets
$\mathcal{N}_r$ Set of branches incident to the from side of cutset r
$\mathcal{G}$ Set of valid cutset states

Indices

i, m, n Nodes.
k, ℓ Branches (non-zero impedance).
τ Contingent topology.
z Breaker (Zero-impedance).
r Substation cutset, consisting of one or more breakers.

Contingent Topology-Dependent Parameters and Variables

For contingent topology τ,

$\mathbf{A}_\tau$ Reduced incidence matrix.
$\mathbf{B}_\tau$ Reduced nodal susceptance matrix with candidate breakers opened.
$\mathbf{f}_\tau$ Vector of real power flows.
$\mathbf{g}_\tau^0$ Bias from linearization of transmission flows.
$\underline{\mathbf{f}}_\tau, \overline{\mathbf{f}}_\tau$ Vectors of transmission limits.
$\underline{\tilde{\mathbf{F}}}_\tau, \overline{\tilde{\mathbf{F}}}_\tau$ Diagonal matrices of transmission limits.
$\mathbf{v}_\tau^{\mathcal{Z}}$ Vector of breaker closing transactions.
$\mathbf{v}_\tau^{\mathcal{S}}$ Vector of flow-cancelling transactions.
$\boldsymbol{\delta}_\tau$ Vector of breaker opening incremental flows (BOIFs).
$\boldsymbol{x}_\tau$ Vector of dummy variables to enforce anti-islanding constraints in the BOIF formulation.
$\boldsymbol{\Psi}_\tau$ Shift factor matrix.
$\boldsymbol{\Phi}_\tau$ PTDF matrix
$\hat{\boldsymbol{\Psi}}_\tau$ Shift factor matrix with candidate breakers removed.
$\hat{\boldsymbol{\Phi}}_\tau$ PTDF matrix with candidate breakers removed
$\hat{\boldsymbol{\Phi}}_\tau^{\mathcal{MZ}}$ PTDF matrix of monitored branches for transfer between the terminals of breakers in a topology with candidate breakers removed (for other set identifier used as superscripts, see discussion in the Nomenclature section).
$\tilde{\boldsymbol{\Phi}}_\tau^{\mathcal{RR}}$ Self-PTDF matrix for cutsets with zero impedances replaced with an arbitrary, constant value.
$\boldsymbol{\Gamma}_\tau$ Matrix of PTDF ratios for cutsets. Columns correspond to cutsets. Rows correspond to monitored branches. All PTDF ratios are with respect to the reference branch for the particular cutset.
$\boldsymbol{\gamma}_\tau^r$ Column vector of $\boldsymbol{\Gamma}_\tau$ corresponding to cutset r
$\boldsymbol{\psi}_\ell$ Row of $\boldsymbol{\Psi}$ for branch ℓ. Individual elements are identified by a node subscript.
ϕ_ℓ^k PTDF of branch ℓ for a transfer across branch k.

Contingent Topology-Independent Parameters and Variables

$\mathbf{1}$	Vector of ones.
$\mathbf{I}$	Identity matrix.
$\tilde{\mathbf{B}}$	Branch susceptance matrix.
$\mathbf{t}^{\mathcal{S}}$	Vector with the 0/1 state of branches
$\mathbf{t}^{\mathcal{Z}}$	Vector with the 0/1 state of breakers
$\mathbf{c}$	Vector of nodal generation variable cost.
$\mathbf{p}$	Vector of nodal generation.
$\mathbf{l}$	Vector of nodal loads.
M	Sufficiently large number.

INTRODUCTION

In recent years there has been a significant interest in co-optimization of transmission topology and generation dispatch in power system operation. Applications have varied from corrective control [1]–[3] to security enhancements [4], [5], loss minimization [6], [7] and more recently to production cost reduction under economic dispatch [8], [9] and unit commitment (UC) [10], [11]. This paper deals with a TC application to production cost minimization in the security-constrained optimal power flow problem (SCOPF). TC can be very effective in this context, as found in [10], [12], [13]. In [14] we introduced a lossless, linear shift factor-based MIP formulation to efficiently model topology control (TC) using flow-cancelling transactions (FCTs) rather than the $B\theta$ representation of power flows. Although $B\theta$ flow modeling is more frequently used in TC research, it is computationally expensive for large systems especially when contingency constraints are included [12], [14]. The FCT-based MIP formulation was extended to include losses in [15].

The majority of TC research has focused on branch and transformer switching. An additional switching action is substation reconfiguration, which consists of opening or closing breakers or switch disconnects not in series with lines or transformers (in the remainder of the paper we will refer to zero-impedance switching devices simply as breakers and to non-zero impedance branches simply as branches). By opening and closing some of these breakers, power flows are re-routed in the transmission network similarly to opening branches. Some substation reconfiguration actions, such as busbar merging or splitting in single-bus substation architectures, can be simpler to implement from an operations perspective. These architectures require as few as a single breaker operation as compared to two breaker operations and two switch disconnect operations to fully connect/disconnect a branch in a typical configuration with a breaker and a disconnect in series with the branch at both ends. More importantly, having the ability to reconfigure substations in combination with branch switching provides additional control mechanisms to system operators for managing congestion in the network.

The busbar merging/splitting problem has been studied [16]–[18] in the context of corrective switching, overload/voltage relief and congestion cost savings. In [16], [19], [20] the authors employ a $B\theta$ formulation of power flows, which has the computational shortcomings mentioned above. In [21] the authors describe a decoupled power flow solution with an exact modeling of breakers and apply it to solve for

active and reactive power system state variables but do not consider switching decisions in an optimization framework. In [3], [17] the authors describe a ranking-based algorithm for busbar and shunt switching based on decoupled power flow and voltage distribution factors that considers both real and reactive power, however, breakers are only modeled approximately by using a very small impedance.

This paper derives a shift factor framework for explicitly and exactly modeling breakers in power flow equations, introduces two TC MIP formulations to optimize substation configuration in the SCOPF problem and presents numerical examples using a real power flow network. By using the shift factor framework to solve TC problems, we aim to achieve faster solution times (especially with contingency constraints) and to be consistent with the type of models used by ISO markets.

The first TC MIP formulation presented in this paper can be thought of as the reverse of the FCT formulation used in branch switching. It starts with a topology where all candidate breakers are open and introduces Breaker Closing Transactions (BCT) to simulate the closing of breakers (in contrast to FCTs, which models opening of non-zero impedance branches). The second formulation starts from a consolidated network topology (bus-branch representation) with all candidate breakers closed and introduces Breaker Opening Incremental Flows (BOIFs) that simulate the opening of breakers. Depending on the state of the topology, the number of candidate substations and the system operator's objectives, one formulation may be more appropriate than the other, as discussed later in this paper.

The rest of this paper is organized in seven sections. Section II derives the shift factor and PTDF matrices for a topology with breakers. Section III discusses the two formulation in the context of typical substation configurations. Section IV uses the developed matrices to formulate the first security-constrained MIP topology control formulation using BCTs and extends the formulation to model branch opening with FCTs. Section V derives BOIFs, applies them to formulate the second security-constrained MIP and extends the formulation to jointly model breaker opening and branch switching. Section VI describes the test system studied and presents results of the BCT, BOIF and joint BOIF+FCT formulations. Section VII discusses some of the data and computational requirements for implementing the BCT and BOIF formulations on a large system. Section VIII presents concluding remarks.

II. DERIVATION OF SENSITIVITIES

To derive appropriate shift factors for a topology with candidate[1] zero-impedance breakers modeled explicitly, we start with a modified set of $B\theta$ constraints.

$$\mathbf{f}_{\tau}^{\mathcal{N}} = \tilde{\mathbf{B}}_{\tau}^{\mathcal{N}} \mathbf{A}_{\tau}^{\mathcal{N}} \theta_{\tau} \tag{1}$$

$$\mathbf{A}_{\tau}^{\mathcal{Z}} \theta_{\tau} = \mathbf{0} \tag{2}$$

$$\mathbf{A}_{\tau}^{\mathcal{N}'} \mathbf{f}_{\tau}^{\mathcal{N}} + \mathbf{A}_{\tau}^{\mathcal{Z}'} \mathbf{f}_{\tau}^{\mathcal{Z}} = \mathbf{l} - \mathbf{p} \tag{3}$$

Equation (1) is the standard loss-less DC powerflow equation for the flow on branches. For breakers, the susceptance is infinity and (1) is undefined, therefore (2) enforces the condition

---
[1]The only breakers modeled are those whose states will be optimized, i.e., *candidate breakers*

that the voltage angle difference between the breaker endpoints is zero. Equation (3) is the nodal balance constraint where we explicitly represent the flow on branches and breakers. To derive shift factor matrices associated with the topology describe above, we take derivatives with respect to the vector of nodal injections

$$\frac{d\mathbf{f}_\tau^{\mathcal{N}}}{d\mathbf{p}} = \frac{d\theta_\tau}{d\mathbf{p}} \mathbf{A}_\tau^{\mathcal{N}'} \tilde{\mathbf{B}}_\tau^{\mathcal{N}} \tag{4}$$

$$\frac{d\theta_\tau}{d\mathbf{p}} \mathbf{A}_\tau^{\mathcal{Z}'} = 0 \tag{5}$$

$$\frac{d\mathbf{f}_\tau^{\mathcal{N}}}{d\mathbf{p}} \mathbf{A}_\tau^{\mathcal{N}} + \frac{d\mathbf{f}_\tau^{\mathcal{Z}}}{d\mathbf{p}} \mathbf{A}_\tau^{\mathcal{Z}} = -\mathbf{I} \tag{6}$$

Substituting (4) into (6) gives

$$\frac{d\theta_\tau}{d\mathbf{p}} \mathbf{A}_\tau^{\mathcal{N}'} \tilde{\mathbf{B}}_\tau^{\mathcal{N}} \mathbf{A}_\tau^{\mathcal{N}} = -\left(\mathbf{I} + \frac{d\mathbf{f}_\tau^{\mathcal{Z}}}{d\mathbf{p}} \mathbf{A}_\tau^{\mathcal{Z}}\right) \tag{7}$$

or

$$\frac{d\theta_\tau}{d\mathbf{p}} = -\left(\mathbf{I} + \frac{d\mathbf{f}_\tau^{\mathcal{Z}}}{d\mathbf{p}} \mathbf{A}_\tau^{\mathcal{Z}}\right) \mathbf{B}_\tau^{-1} \tag{8}$$

The nodal susceptance matrix $\mathbf{B}_\tau$ in (8) is for the topology with all candidate breakers open and is well defined as long as opening all candidate breakers does not island any part of the system under contingency τ. Substation networks formed by non-candidate, closed, breakers can be collapsed and treated as a single bus. Substituting (8) into (5) gives

$$\mathbf{\Psi}_\tau^{\mathcal{Z}} = \left(\frac{d\mathbf{f}_\tau^{\mathcal{Z}}}{d\mathbf{p}}\right)' = -\left(\mathbf{A}_\tau^{\mathcal{Z}} \mathbf{B}_\tau^{-1} \mathbf{A}_\tau^{\mathcal{Z}'}\right)^{-1} \mathbf{A}_\tau^{\mathcal{Z}} \mathbf{B}_\tau^{-1} \tag{9}$$

Equation (9) defines the shift factor matrix for breakers, assuming that the inverse on the right hand side exists. Assuming for now that it does, we expand (4) using (8)

$$\mathbf{\Psi}_\tau^{\mathcal{N}} = \left(\frac{d\mathbf{f}_\tau^{\mathcal{N}}}{d\mathbf{p}}\right)' = -\tilde{\mathbf{B}}_\tau^{\mathcal{N}} \mathbf{A}_\tau^{\mathcal{N}} \mathbf{B}_\tau^{-1} \left(\mathbf{I} + \mathbf{A}_\tau^{\mathcal{Z}'} (\frac{d\mathbf{f}_\tau^{\mathcal{Z}}}{d\mathbf{p}})'\right) \tag{10}$$

Equation (10) is the shift factor matrix for monitored branches where the first term on the right hand side,

$$\hat{\mathbf{\Psi}}_\tau = -\tilde{\mathbf{B}}_\tau^{\mathcal{N}} \mathbf{A}_\tau^{\mathcal{N}} \mathbf{B}_\tau^{-1} \tag{11}$$

is the shift factor matrix with all candidate breakers open.

The matrix in (9) is invertible when $\mathbf{A}_\tau^{\mathcal{Z}}$ is of maximal rank and when there are no islands in the system with candidate breakers open. Under the latter assumption the nodal susceptance matrix is a positive definite symmetric matrix [22] and together with the first assumption, the matrix in (9) is invertible [23]. For the incidence matrix $\mathbf{A}_\tau^{\mathcal{Z}}$ to be of maximal rank, the network should not have any parallel breakers or closed loops formed by breakers. Parallel breakers can be handled ex-post, but most types of substations do contain loops. In the next section we demonstrate on typical substation configurations that formulating both the BCT and BOIF formulations using a bus-branch representation with virtual breakers avoids all issues with loops and parallel breakers.

To close this section we derive the impact of closing breakers on the rest of the system, which we will use in the BCT MIP formulation. This impact is the *line closing distribution factor* (LCDF) and is defined by $d\mathbf{f}_\tau^{\mathcal{N}}/d\mathbf{f}_\tau^{\mathcal{Z}}$. Differentiating (1) - (3) with respect to $\mathbf{f}_\tau^{\mathcal{Z}}$,

$$\frac{d\mathbf{f}_\tau^{\mathcal{N}}}{d\mathbf{f}_\tau^{\mathcal{Z}}} = \frac{d\theta_\tau}{d\mathbf{f}_\tau^{\mathcal{Z}}} \mathbf{A}_\tau^{\mathcal{N}'} \tilde{\mathbf{B}}_\tau^{\mathcal{N}} \tag{12}$$

$$\frac{d\theta_\tau}{d\mathbf{f}_\tau^{\mathcal{Z}}} \mathbf{A}_\tau^{\mathcal{Z}'} = 0 \tag{13}$$

$$\frac{d\mathbf{f}_\tau^{\mathcal{N}}}{d\mathbf{f}_\tau^{\mathcal{Z}}} \mathbf{A}_\tau^{\mathcal{N}} + \mathbf{A}_\tau^{\mathcal{Z}} = 0 \tag{14}$$

Taking a similar set of steps as for the derivation of $\mathbf{\Psi}_\tau^{\mathcal{N}}$

$$\left(\frac{d\mathbf{f}_\tau^{\mathcal{N}}}{d\mathbf{f}_\tau^{\mathcal{Z}}}\right)' = -\tilde{\mathbf{B}}_\tau^{\mathcal{N}} \mathbf{A}_\tau^{\mathcal{N}} \left(\mathbf{A}_\tau^{\mathcal{N}'} \tilde{\mathbf{B}}_\tau^{\mathcal{N}} \mathbf{A}_\tau^{\mathcal{N}}\right)^{-1} \mathbf{A}_\tau^{\mathcal{Z}'}$$
$$= \left(\hat{\mathbf{\Psi}}_\tau\right) \mathbf{A}_\tau^{\mathcal{Z}'} = \left(\hat{\mathbf{\Phi}}_\tau^{\mathcal{N}Z}\right) \tag{15}$$

where $\hat{\mathbf{\Psi}}$ and $\hat{\mathbf{\Phi}}$ refer to the topology with candidate breakers opened. The LCDF in (15) can be used to emulate the closing of a breaker by an injection and withdrawal at its terminals.

We have shown in this section that we can define a set of shift factors and LCDFs in a topology containing zero-impedance breakers. In the next section we review some typical substation configurations and discuss the topology representation used in both shift factor based MIP formulations

III. TYPICAL SUBSTATIONS AND VIRTUAL BREAKERS

In the shift factor formulations used in this paper we effectively work with a bus-branch representation of the network, consolidating non-candidate nodes, busbars and breakers into their equivalent bus. Fig. 1 shows a typical breaker-and-a-half substation architecture. Let us consider two possible
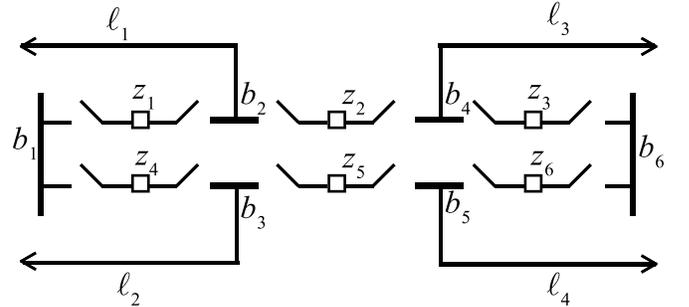

Fig. 1. Breaker-and-a-half substation architecture with branches labeled as ℓ_1 through ℓ_4, busbars b_1 and b_6, nodes b_2 through b_5 and breakers z_1 through z_6.

reconfiguration states: a) z_2, z_5 are open and b) z_1, z_6 are open (all other breakers are closed). While the BCT and BOIF formulations evaluate these reconfiguration decisions differently, both view the network as one of the bus-branch representation shown in Fig. 2, with a single virtual breaker. In the BCT formulation, the initial state of the system would typically have breakers z_2, z_5 or z_1, z_6 disconnected (Figures 2a and 2b respectively) and would evaluate the benefits of closing the virtual breaker, i.e., reconnecting one of the pairs of breakers. In the BOIF formulation, on the other hand, the substation may start out fully connected and the formulation would dynamically evaluate both switching decisions in Fig.
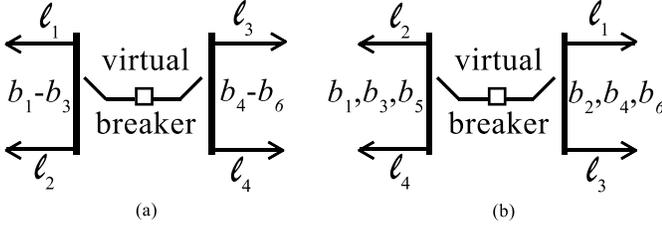
Fig. 2. Bus-branch representation of a breaker-and-a-half substation. Opening the virtual breaker in (a) corresponds to opening breakers z_2, z_5 in Fig. 1, consolidating nodes b_2 and b_3 into busbar b_1 and nodes b_4 and b_5 into busbar b_6. Opening the virtual breaker in (b) corresponds to opening breakers z_1, z_6 in Fig. 1, consolidating nodes b_3 and b_5 into busbar b_1 and nodes b_2 and b_4 into busbar b_6.

2 (constraints to prevent mutually exclusive decisions would be added). Similar logic applies for the single bus with a breaker tie configuration shown in Fig. 3, where breaker tie z_1 already acts as a virtual breaker. Further, in Fig. 3 we make
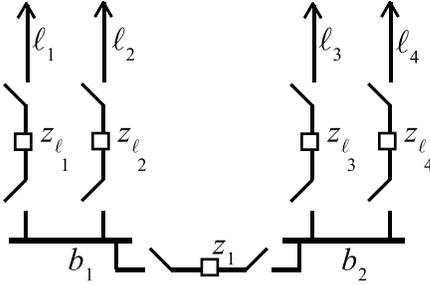

Fig. 3. Single bus with a breaker tie configuration with branches labeled as ℓ_1 through ℓ_4, busbars b_1 and b_2, breaker tie z_1 and other breakers z_{ℓ_1} through z_{ℓ_4}.

the distinction between substation reconfiguration and branch switching, represented by breakers z_{ℓ_1} through z_{ℓ_4}. While both types of switching actions require breaker operations, the physical implications are quite different. In Section V we use the single bus and ring bus configurations to show that modeling breaker opening requires a different approach from branch switching.

The next two sections derive the BCT and BOIF formulations. Regardless of the formulation, however, using a consolidated representation of the topology with virtual breakers avoids the issue of breaker loops and ensures that the sensitivities derived in the previous section are well defined.

IV. MIP FORMULATIONS WITH BCTs

Many aspects of the breaker closing formulation are similar to the FCT formulation for branch switching [14]. In this section we apply sensitivities from Section II to formulate the breaker closing MIP and the joint breaker closing and branch opening MIP.

A. BCT MIP Formulation

To formulate the BCT MIP we need to determine the magnitude of the breaker closing transactions when $z_\ell = 1$. There are two ways to determine this magnitude. From the shift factors derived in the previous section, the flow on closed breakers is

$$\mathbf{f}_\tau^{\mathcal{Z}} = \mathbf{\Psi}_\tau^{\mathcal{Z}}(\mathbf{p}-\mathbf{l}) - (\mathbf{A}_\tau^{\mathcal{Z}}\mathbf{B}_\tau^{-1}\mathbf{A}_\tau^{\mathcal{Z}'})^{-1}\mathbf{A}_\tau^{\mathcal{Z}}\mathbf{B}_\tau^{-1}(\mathbf{p}-\mathbf{l}) \quad (16)$$

from which we can write

$$\left(\mathbf{A}_\tau^{\mathcal{Z}}\mathbf{B}_\tau^{-1}\mathbf{A}_\tau^{\mathcal{Z}'}\right)\mathbf{f}_\tau^{\mathcal{Z}} + \mathbf{A}_\tau^{\mathcal{Z}}\mathbf{B}_\tau^{-1}(\mathbf{p}-\mathbf{l}) = 0 \quad (17)$$

Alternatively, from the $B\theta$ formulation, we know that the angle difference across breakers is 0. When $z = 1$, we impose this requirement in the shift factor formulation by appropriately setting the decision variable $\mathbf{p}$. By applying (5)

$$\mathbf{A}_\tau^{\mathcal{Z}}\frac{d\theta_\tau'}{d\mathbf{p}}(\mathbf{p}-\mathbf{l}) = 0 \quad (18)$$

Expanding out the terms using (8), we have

$$-\mathbf{A}_\tau^{\mathcal{Z}}\mathbf{B}_\tau^{-1}(\mathbf{I} + \mathbf{A}_\tau^{\mathcal{Z}'}\mathbf{\Psi}_\tau^{\mathcal{Z}})(\mathbf{p}-\mathbf{l}) =$$
$$\mathbf{A}_\tau^{\mathcal{Z}}\mathbf{B}_\tau^{-1}(\mathbf{p}-\mathbf{l}) + \mathbf{A}_\tau^{\mathcal{Z}}\mathbf{B}_\tau^{-1}\mathbf{A}_\tau^{\mathcal{Z}'}\mathbf{v}_\tau^{\mathcal{Z}} = 0 \quad (19)$$

Equations (17) and (19) are identical, where the BCT, $\mathbf{v}_\tau^{\mathcal{Z}}$ is precisely the flow on closed breakers given by

$$\mathbf{v}_\tau^{\mathcal{Z}} = \mathbf{\Psi}_\tau^{\mathcal{Z}}(\mathbf{p}-\mathbf{l}) \quad (20)$$

Using (19) we now formulate the SCOPF BCT MIP as follows

$$\mathcal{C} = \min_{\mathbf{p},\mathbf{v},\mathbf{t}} \mathbf{c}'\mathbf{p} \quad (21)$$

$$\text{s.t.} \quad \mathbf{1}'(\mathbf{p}-\mathbf{l}) = 0 \quad (22)$$

$$\underline{\mathbf{p}} \leq \mathbf{p} \leq \overline{\mathbf{p}} \quad (23)$$

$$\underline{\mathbf{f}}_\tau^{\mathcal{M}} \leq \mathbf{g}_\tau^0 + \hat{\mathbf{\Psi}}_\tau^{\mathcal{M}}(\mathbf{p}-\mathbf{l}) - \hat{\mathbf{\Phi}}_\tau^{\mathcal{M}\mathcal{Z}}\mathbf{v}_\tau^{\mathcal{Z}} \leq \overline{\mathbf{f}}_\tau^{\mathcal{M}} \quad \forall\tau \quad (24)$$

$$-M(\mathbf{1}-\mathbf{t}^{\mathcal{Z}}) \leq \left(\mathbf{A}_\tau^{\mathcal{Z}}\mathbf{B}_\tau^{-1}\mathbf{A}_\tau^{\mathcal{Z}'}\right)\mathbf{v}_\tau^{\mathcal{Z}} +$$
$$\mathbf{A}_\tau^{\mathcal{Z}}\mathbf{B}_\tau^{-1}(\mathbf{p}-\mathbf{l}) \leq M(\mathbf{1}-\mathbf{t}^{\mathcal{Z}}) \quad \forall\tau \quad (25)$$

$$-M\mathbf{t}^{\mathcal{Z}} \leq \mathbf{v}_\tau \leq M\mathbf{t}^{\mathcal{Z}} \quad \forall\tau \quad (26)$$

$$\mathbf{t}^{\mathcal{Z}} \in \{0,1\} \quad (27)$$

Equations (21) - (24) are identical in structure to the branch switching formulation.[2] Specifically, (24) enforces the flows on monitored branches, which are impacted by all BCTs. Equations (25) and (26) force the flow on breakers to (16) when $t^{\mathcal{Z}} = 1$ and otherwise leave (25) unconstrained. One complication in this formulation is that equations (24) and (25) rely on calculating $\mathbf{B}_\tau^{-1}$ for every contingent topology τ. However, the number of changes in $\mathbf{B}$ introduced by a contingency are limited. For single element contingencies outaging branch ℓ, the update of the form

$$\mathbf{B}_\tau^{-1} = (\mathbf{B}_0 - \frac{1}{b_\ell}\mathbf{u}\mathbf{u}')^{-1} \quad (28)$$

can be computed quickly and efficiently using the matrix inversion lemma. Note that the solution of (21) - (27) is secure

---

[2]The sign difference on the PTDF matrix in (24) arises because we are simulating branch closing as opposed to branch opening distribution factors.

against all specified contingencies with constraints (24) modeling post-contingency flow limitations for each contingent topology τ

B. Joint BCT and FCT MIP Formulation

Including FCTs in (21)-(27) requires a few small changes. We first need to introduce $\mathbf{v}_\tau^{\mathcal{S}}$ and $\mathbf{t}^{\mathcal{S}}$ to represent FCTs and the binary branch switching variables. Constraints (26) would be introduced for FCTs and the term $\hat{\boldsymbol{\Phi}}_\tau^{\mathcal{MS}}\mathbf{v}_\tau^{\mathcal{S}}$ would be added to (24). Equation (25) would change since the flow on breakers would now be impacted by FCTs:

$$\mathbf{f}_\tau^{\mathcal{Z}} = -\left(\mathbf{A}_\tau^{\mathcal{Z}}\mathbf{B}_\tau^{-1}\mathbf{A}_\tau^{\mathcal{Z}'}\right)^{-1}\mathbf{A}_\tau^{\mathcal{Z}}\mathbf{B}_\tau^{-1}(\mathbf{p}-\mathbf{l})+\hat{\boldsymbol{\Phi}}_\tau^{\mathcal{ZS}}\mathbf{v}_\tau^{\mathcal{S}} \quad (29)$$

By multiplying both sides by the invertible matrix on the right hand side and collecting terms we arrive at

$$\mathbf{A}_\tau^{\mathcal{Z}}\mathbf{B}_\tau^{-1}\left(\mathbf{A}_\tau^{\mathcal{Z}'}\mathbf{f}_\tau^{\mathcal{Z}} + (\mathbf{p}-\mathbf{l}) - \mathbf{A}_\tau^{\mathcal{Z}'}\hat{\boldsymbol{\Phi}}_\tau^{\mathcal{MS}}\mathbf{v}_\tau^{\mathcal{S}}\right) = 0 \quad (30)$$

Equations (31)-(37) define the security constrained MIP formulation with both forms of topology control actions:

$$\mathcal{C} = \min_{\mathbf{p},\mathbf{v},\mathbf{t}} \mathbf{c}'\mathbf{p} \quad (31)$$

$$\text{s.t.} \quad (22), (23), (26) \quad (32)$$

$$\underline{\mathbf{f}}_\tau^{\mathcal{M}} \le \mathbf{g}^0 + \hat{\boldsymbol{\Psi}}_\tau^{\mathcal{M}}(\mathbf{p}-\mathbf{l})-\hat{\boldsymbol{\Phi}}_\tau^{\mathcal{MZ}}\mathbf{v}_\tau^{\mathcal{Z}} + \hat{\boldsymbol{\Phi}}_\tau^{\mathcal{MS}}\mathbf{v}_\tau^{\mathcal{S}} \le \overline{\mathbf{f}}_\tau^{\mathcal{M}} \quad (33)$$

$$\underline{\tilde{\mathbf{F}}}_\tau\mathbf{t}^{\mathcal{S}} \le \hat{\boldsymbol{\Psi}}_\tau^{\mathcal{S}}(\mathbf{p}-\mathbf{l}) + \left(\hat{\boldsymbol{\Phi}}_\tau^{\mathcal{SS}}-\mathbf{I}\right)\mathbf{v}_\tau^{\mathcal{S}}-\hat{\boldsymbol{\Phi}}_\tau^{\mathcal{SZ}}\mathbf{v}_\tau^{\mathcal{Z}} \le \overline{\tilde{\mathbf{F}}}_\tau\mathbf{t}^{\mathcal{S}} \quad (34)$$

$$-M(\mathbf{1} - \mathbf{t}^{\mathcal{Z}}) \le \mathbf{A}_\tau^{\mathcal{Z}}\mathbf{B}_\tau^{-1}\left(\mathbf{A}_\tau^{\mathcal{Z}'}\mathbf{v}_\tau^{\mathcal{Z}} + (\mathbf{p}-\mathbf{l})-\right.$$
$$\left.\mathbf{A}_\tau^{\mathcal{Z}'}\hat{\boldsymbol{\Phi}}_\tau^{\mathcal{MS}}\mathbf{v}_\tau^{\mathcal{S}}\right) \le M(\mathbf{1} - \mathbf{t}^{\mathcal{Z}}) \quad (35)$$

$$-M(\mathbf{1} - \mathbf{t}^{\mathcal{S}}) \le \mathbf{v}_\tau^{\mathcal{S}} \le M(\mathbf{1} - \mathbf{t}^{\mathcal{S}}) \quad (36)$$

$$\mathbf{t}^{\mathcal{Z}}, \mathbf{t}^{\mathcal{S}} \in \{0,1\} \quad (37)$$

Equation (34) forces the flow on opened branches to zero. The formulation above models both branch switching and breaker closing in a single optimization problem.

We now shift focus to the second MIP formulation that starts with all breakers closed and models breaker opening using flow sensitivities.

V. Breaker Opening MIP Formulations

To formulate a linear shift factor-based OPF that emulates the opening of breakers we would like to use FCTs. Unfortunately, the use of FCTs creates two problems. In the branch opening formulation we isolate the branch to be opened and introduce a FCT, v, at the ends of this branch, which has the same impact on the rest of the system as actually opening the branch. The algorithm determines v by dynamically calculating the LODF, which requires evaluating $(\mathbf{I} - \boldsymbol{\Phi}^{\mathcal{SS}})^{-1}$. For breakers this expression is undefined due to the breakers' zero impedance.

The second problem arises from the impact of FCTs on the rest of the system. Due to the self-PTDF being undefined, we cannot introduce FCTs at the ends of the breakers whose opening we want to emulate. If we try to introduce FCTs at any other nodes in the system we would inadvertently impact nodal balance constraints. The two problems preclude the use

of FCTs for emulating the opening of breakers. To get around these issues we work directly with fictitious flows that we call Breaker Opening Incremental Flows (BOIFs).

A. BOIF Theory

The BOIF δ_ℓ^z is a fictitious flow introduced on branch ℓ, in a topology where the virtual breaker z is connected (see Fig. 2). It is defined as the change in flow on branch ℓ when z is disconnected (similarly to a LODF) but, as explained below, avoids the problem of the self-PTDF being undefined. Additionally, fictitious flows do not create any nodal injections and therefore avoid the issue with the nodal balance constraints described above.

To show that BOIFs are well defined, consider virtual breaker z defined from node i to j, expressed as $z = (i, j)$. For any pair of branches incident to virtual breaker z, $\ell = (m, i)$ and $k = (n, i)$ the per-unit impact on the flow of these branches from opening z is the LODF.

$$\Delta f_\ell^z = LODF_\ell^z \quad (38)$$
$$\Delta f_k^z = LODF_k^z \quad (39)$$

As stated earlier, the LODF for a breaker is undefined. However, we claim that the ratio of (38) to (39),

$$\frac{\Delta f_\ell^z}{\Delta f_k^z} = \frac{LODF_\ell^z}{LODF_k^z} = \frac{\phi_\ell^z}{\phi_k^z} \quad (40)$$

is well defined and independent of the impedance (and therefore susceptance) of z. We leave the proof for the appendix and show in the next section that we can find fictitious incremental flows for all branches incident to z that emulate the opening of breaker z. Further, these BOIFs impact the rest of the system in the same way as physically opening z. Note that in the final result of (40) we canceled the $(1 - \phi_z^z)$ terms from both numerator and denominator. We return to this point in the next section.

B. BOIF MIP Formulation

Using the ratio of incremental flows derived in the previous section, we can formulate a shift factor based MIP OPF to optimize the opening of breakers. We can think of opening a zero-impedance breaker as separating busbars as motivated by Fig. 2. In the single bus substation (shown again in Fig.
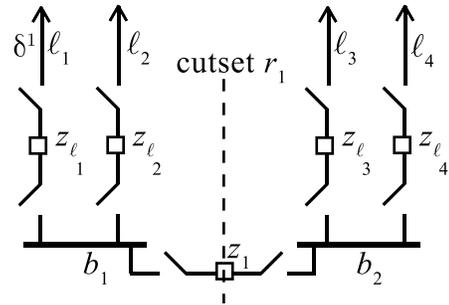

Fig. 4. Single bus with a breaker tie substation. A cutset is introduced with an associated BOIF variable δ^{r_1}

4), if we open breaker z_1, we introduce a substation cutset,

r_1, shown by the dashed line and separate busbar b_2 from the rest of the substation (in this case we also separate busbar b_1). From the previous section we know that to find the impact of opening z on the rest of the system, we must consider the relative changes in flow for any pair of branches. Applying this result, we introduce a BOIF variable, $\delta^r = \Delta f_{\ell_1}^z$ representing the change in flow on ℓ_1 when cutset r_1 is opened. We call ℓ_1 the reference branch and calculate the changes in flow on branches incident to the from-node of breaker z.

From (40) we have:

$$\delta_k^{r_1} = \delta^{r_1} \frac{\phi_k^z}{\phi_{\ell_1}^z} = \delta^{r_1} \gamma_k^r \qquad k = \ell_2 \tag{41}$$

Equation (41) establishes a relationship between changes in flows that would result from the opening of virtual breaker z. In addition, we need to determine the magnitude of δ^{r_1}. In the post-open topology, the sum of flows through branches ℓ_1 and ℓ_2 is zero. In the pre-open topology the BOIF emulates this condition, expressed by (42).[3]

$$-Mt_{r_1} \leq \sum_{\ell \in (\ell_1, \ell_2)} \left(\boldsymbol{\psi}_\ell(\mathbf{p}-\mathbf{l}) + \delta^{r_1} \gamma_k^{r_1} \right) + l_1 - p_1 \leq Mt_{r_1} \tag{42}$$

Constraint (42) enforces the nodal balance for busbar b_1 in the pre-open network, except that we replace the flow through z with the fictitious breaker opening incremental flows (BOIFs) that emulate its opening. Note that (42) only balances one of the two busbars separated. This is a sufficient condition. If the flow through ℓ_1 and ℓ_2 is 0, the flow through ℓ_3 and ℓ_4 will naturally satisfy the same condition. The previous example illustrates the constraints required to model the opening of a single cutset (breaker). In the rest of this section we expand these constraints to allow for multiple cutsets.

Fig. 5 shows a ring bus configuration but the same principle applies to a breaker-and-a-half configuration. For the ring bus
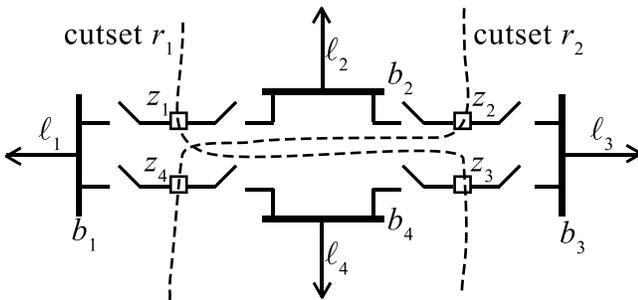

Fig. 5. Ring bus configuration with branches labeled as ℓ_1 through ℓ_4, nodes b_1 through b_4, breakers z_1 through z_4 and two possible cutsets, r_1 and r_2.

shown, opening any single breaker has no impact on the rest of the system. By introducing the two cutsets, r_1 and r_2, the BOIF formulation will dynamically evaluate the two states shown in Fig. 2. Opening cutset r_1 corresponds to opening the virtual breaker in Fig. 2a (nodes b_1 and b_4 would be on the left side of the virtual breaker) and opening cutset r_2 correponds to opening the virtual breaker in Fig. 2b (nodes b_1 and b_2

[3]Without loss of generality, (42) assumes that all branches incident to the from-busbar b_1 of breaker z are defined as originating at busbar 1.

would be on the left side of the virtual breaker). For cutset r_1 in Fig. 5, (42) becomes:

$$-Mt_{r_1} \leq \sum_{\ell \in (\ell_1, \ell_2)} \left(\boldsymbol{\psi}_\ell(\mathbf{p} - \mathbf{l}) + \delta^{r_1} \gamma_\ell^{r_1} + \delta^{r_2} \gamma_\ell^{r_2} \right)$$
$$+ l_{r_1} - p_{r_1} \leq Mt_{r_1} \tag{43}$$

where l_r and p_r refer to load and generation at the from side of cutset r.[4] Note that we only consider the reference branch for r_2 when calculating the impact on the nodal balance constraint for r_1. To see that this is indeed the case, consider an arbitrary set of injections that cause a δ_k change in the flow on some branch, k. We can use shift factors to calculate their impact on any other branch, ℓ but we can also use PTDFs and δ_k directly to get the same result. In Section III we mentioned that some substations reconfigurations may be mutually exclusive. For example, if opening both cutsets in the ring bus is prohibited, a simple constraint limiting the sum of the binary values to be less than or equal to 1 can be added. More generally, we can say that the vector $\mathbf{t}$ should belong to the set of valid cutset states $\mathcal{G}$, which we assume to be known by the system operator.

Extending (43) to multiple cutsets and changing to matrix notation we have

$$-Mt_r \leq \mathbf{1}'_{\ell \in \mathcal{N}_r} (\boldsymbol{\Psi}_\tau(\mathbf{p}-\mathbf{l}) + \boldsymbol{\Gamma}_\tau \boldsymbol{\delta}_\tau) \tag{44}$$
$$+ (l_r - p_r) \leq Mt_r \; \forall r, \tau$$

Before we present the full BOIF formulation, we need additional constraints to prevent islanding. We noted in Section V that in calculating (40) we cancel the terms $(1 - \phi_z^z)$ from both numerator and denominator. This cancellation works as long as the cutset being opened does not create islands. More generally, a set of cutsets is non-islanding if the term $(\mathbf{I} - \boldsymbol{\Phi}^{\mathcal{R}\mathcal{R}})$ is invertible. In the FCT formulation this condition is implicitly captured by (34) and (36), repeated below without the impact of breakers (for clarity).

$$\underline{\tilde{\mathbf{F}}}_\tau \mathbf{t}^\mathcal{S} \leq \boldsymbol{\Psi}_\tau^\mathcal{S}(\mathbf{p}-\mathbf{l}) + \left(\boldsymbol{\Phi}_\tau^{\mathcal{S}\mathcal{S}} - \mathbf{I} \right) \mathbf{v}_\tau \leq \overline{\tilde{\mathbf{F}}}_\tau \mathbf{t}^\mathcal{S} \; \forall \tau \tag{45}$$
$$-M(\mathbf{1}-\mathbf{t}^\mathcal{S}) \leq \mathbf{v}_\tau^\mathcal{S} \leq M(\mathbf{1}-\mathbf{t}^\mathcal{S}) \; \forall \tau \tag{46}$$

For branches that are switched open ($\mathbf{t}^\mathcal{S} = 0$), we see that solving for $\mathbf{v}_\tau$ in (45) requires inverting $\left(\mathbf{I} - \boldsymbol{\Phi}_\tau^{\mathcal{S}\mathcal{S}} \right)$. In the BOIF formulation, we need to explicitly add a similar constraint. Even though the impedance of breakers is zero, we only care about network connectivity and therefore can substitute all breaker impedances with an arbitrary value. We refer to the PTDF matrix post these substitutions as $\tilde{\boldsymbol{\Phi}}$ and the additional anti-islanding constraints are shown in (47)-(48)

$$-Mt_r + \mathbf{1} \leq (\mathbf{I} - \tilde{\boldsymbol{\Phi}}_\tau^{\mathcal{R}\mathcal{R}})\mathbf{x}_\tau \leq Mt_r + \mathbf{1} \; \forall \tau, r \tag{47}$$
$$-M(1 - t_r) \leq \mathbf{x}_\tau \leq M(1 - t_r) \; \forall \tau, r \tag{48}$$

Where $\mathbf{x}_\tau$ is a vector of dummy variables coupled to the binary decision variables $\mathbf{t}$, and allows us to determine whether the submatrix of $(\mathbf{I} - \tilde{\boldsymbol{\Phi}}_\tau^{\mathcal{R}\mathcal{R}})$ corresponding to cutsets where $r = 0$

[4]For the substation reconfigurations in this paper, we assume that the location of the generation and load within a substation is fixed or that it is implicitly adjusted for the configuration being considered.

is invertible[5]. We are now ready to present the full security-constrained BOIF MIP formulation

$$\mathcal{C} = \min_{\mathbf{p},\boldsymbol{\delta},\boldsymbol{x},\mathbf{t}} \mathbf{c}'\mathbf{p} \tag{49}$$

$$\text{s.t. } (22),\,(23),\,(44),\,(47),\,(48) \tag{50}$$

$$\underline{\mathbf{f}}_\tau^{\mathcal{M}} \le \mathbf{g}_\tau^0 + \boldsymbol{\Psi}_\tau^{\mathcal{M}}\,(\mathbf{p} - \mathbf{l}) + \boldsymbol{\Gamma}_\tau^{\mathcal{M}}\boldsymbol{\delta}_\tau \le \overline{\mathbf{f}}_\tau^{\mathcal{M}} \quad \forall \tau \tag{51}$$

$$-M(1 - t_r^{\mathcal{Z}}) \le \boldsymbol{\delta}_\tau \le M(1 - t_r^{\mathcal{Z}}) \quad \forall r,\tau \tag{52}$$

$$\mathbf{t}^{\mathcal{Z}} \in \{0,1\},\, \mathbf{t}^{\mathcal{Z}} \in \mathcal{G} \tag{53}$$

C. Joint BOIF and FCT MIP Formulation

For completeness, we present the joint formulation for breaker and branch switching.

$$\mathcal{C} = \min_{\mathbf{p},\boldsymbol{\delta},\boldsymbol{x},\mathbf{t}^{\mathcal{Z}},\mathbf{t}^{\mathcal{S}},\boldsymbol{v}} \mathbf{c}'\mathbf{p} \tag{54}$$

$$\text{s.t. } (22),\,(23),\,(36),\,(47),\,(48),\,(52) \tag{55}$$

$$\underline{\mathbf{f}}_\tau^{\mathcal{M}} \le \mathbf{g}_\tau^0 + \boldsymbol{\Psi}_\tau^{\mathcal{M}}\,(\mathbf{p} - \mathbf{l})$$
$$+ \boldsymbol{\Gamma}_\tau^{\mathcal{M}}\boldsymbol{\delta}_\tau + \boldsymbol{\Phi}_\tau^{\mathcal{M}\mathcal{S}}\mathbf{v}_\tau \le \overline{\mathbf{f}}_\tau^{\mathcal{M}} \quad \forall \tau \tag{56}$$

$$-Mt_r \le \mathbf{1}'_{\ell \in \mathcal{N}_r}\Big(\boldsymbol{\Psi}_\tau(\mathbf{p} - \mathbf{l}) + \boldsymbol{\Gamma}_\tau\boldsymbol{\delta}_\tau + \boldsymbol{\Phi}_\tau^{\mathcal{M}\mathcal{S}}\mathbf{v}_\tau\Big)$$
$$+ (l_r - p_r) \le Mt_r \quad \forall r,\tau \tag{57}$$

$$\underline{\tilde{\mathbf{F}}}_\tau\mathbf{t}^{\mathcal{S}} \le \boldsymbol{\Psi}_\tau^{\mathcal{S}}\,(\mathbf{p} - \mathbf{l}) + \big(\boldsymbol{\Phi}_\tau^{\mathcal{S}\mathcal{S}} - \mathbf{I}\big)\mathbf{v}_\tau + \boldsymbol{\Gamma}_\tau^{\mathcal{S}}\boldsymbol{\delta}_\tau \le \overline{\tilde{\mathbf{F}}}_\tau\mathbf{t}^{\mathcal{S}} \quad \forall \tau \tag{58}$$

$$\mathbf{t}^{\mathcal{Z}}, \mathbf{t}^{\mathcal{S}} \in \{0,1\},\, \mathbf{t}^{\mathcal{Z}} \in \mathcal{G} \tag{59}$$

Equation (57) assumes that branches incident to cutsets are in the monitored set but this need not be the case. Formulation (54)-(59) starts from the original topology and allows for reconfiguration of substations and branch switching within a single MIP formulation.

VI. NUMERICAL EXPERIMENTS

A. Test System

The test system used represents 168 hours in a historical 2013 week of a subarea of PJM. Each hour was modeled independently with the assumption that each breaker can be opened/reclosed in each hour. The system can be further characterized as follows:

- 2,264 branches (298 monitored)
- 4 contingency constraints of interest
- 2,034 nodes
- 63 generators
- The hourly loads and generator commitment schedules are taken from archived system snapshots
- The generation costs are taken from the real-time market
- Switching costs are added to the objective cost of all formulations with the aim of differentiating the objective function under solution degeneracy conditions.[6]

Out of all breakers, we identified 57 whose opening would split a bus. In the test system used, all 57 breakers could not be opened at the same time without splitting the system.

[5]Each column and row in $\tilde{\boldsymbol{\Phi}}_\tau^{\mathcal{R}\mathcal{R}}$ corresponds to a single virtual breaker as shown in Fig. 2.

[6]These switching costs could be negative depending on the preference of the system operator, for example to bias the MIP solution towards keeping a branch open from one hour to the next.

Therefore, we selected a subset of 39 switchable breakers that do not island the system when opened simultaneously. Since all candidate breakers are open under the BCT formulation, the remaining substations can be collapsed into their representative buses and this significantly reduces the number of breakers modeled explicitly. After performing this consolidation, the model size is reduced to 406 branches and 310 buses. In the BOIF formulation we could use all 57 candidate breakers as decision variables. However, for comparability of results with the BCT formulation we maintain the same 39 candidates for both formulations.

In addition to modeling the BOIF and BCT formulations we also model the FCT formulation and provide results for the joint BOIF and FCT formulation. Since there are over 400 branches in the reduced test system, we cannot consider all of them as switchable. Prior to running the FCT model we evaluate the line profit policy to determine a set of candidate branches (the details of this policy can be found in [13], [24]). For each hour, the line profit policy performs the following steps:

1) Rank branches using metric $-f_\ell(LMP_{\ell_{To}} - LMP_{\ell_{From}})$.
2) Open top-ranked branch (having a negative metric) and solve OPF.
3) Compare post-open to pre-open production costs. If there is an improvement, keep branch from step 2 open in all future iterations and go to step 1. Otherwise keep branch from step 2 closed. If no more candidates exist, end and go to the next hour.

This algorithm generated six candidate branches for the week simulated, which were included in the switchable set for each hourly MIP model. Note that there may be other branches whose opening would produce savings but our goal here is to quickly generate a reasonable switchable set.

In evaluating the performance of the BCT, BOIF and joint BOIF+FCT formulation, the next section presents results comparing the number of topology control actions across the models as well as solution times and cost savings. Cost savings are calculated relative to the maximum possible savings to make the comparison across hours more consistent using the following relative cost of congestion metric:

$$\%savings = \frac{\mathcal{C}^{full\ topology} - \mathcal{C}^{optimized\ topology}}{\mathcal{C}^{full\ topology} - \mathcal{C}^{no\ constraints\ topology}} \tag{60}$$

where $\mathcal{C}^{full\ topology}$ corresponds to production costs for a system before any switching actions are applied and $\mathcal{C}^{no\ constraints\ topology}$ corresponds to production costs for a system with no transmission constraints enforced. All of the modeling was implemented in AIMMS 3.12 using CPLEX 12.5 with default settings. Simulations were run on a 64-bit workstation with two 2.93 GHz Intel Xeon processors (8 cores total) and 24 GB of RAM. Because the size of the system is relatively small we are able to solve both models to the global optimal (MIP gap of 0%). A value of 5,000 was used for M in the formulations. In practice, the value for M is chosen to be constraint-specific, reflecting the physics of the system. This would provide tighter bounds on the feasible space and improve solver performance. Alternatively, the authors in [25] present an approach for solving transmission switching

problems without big-M constraints by describing the convex hull relaxation of the feasible space and introducing strong inequalities that could be used in a cutting-planes approach for solving these problems.

B. Simulation Results

We begin by showing a simple example of substation reconfiguration using the test system. Fig. 6 shows a small part of the full test system where branch ℓ_k (between nodes b_4 and b_5) carries its maximum flow with all breakers closed. Part of the flow through ℓ_k goes from the rest of the network along path $b_5-b_4-b_3-b_2-b_1$ and serves to meet the load at b_1. With breaker z_1 opened (without redispatch), the original
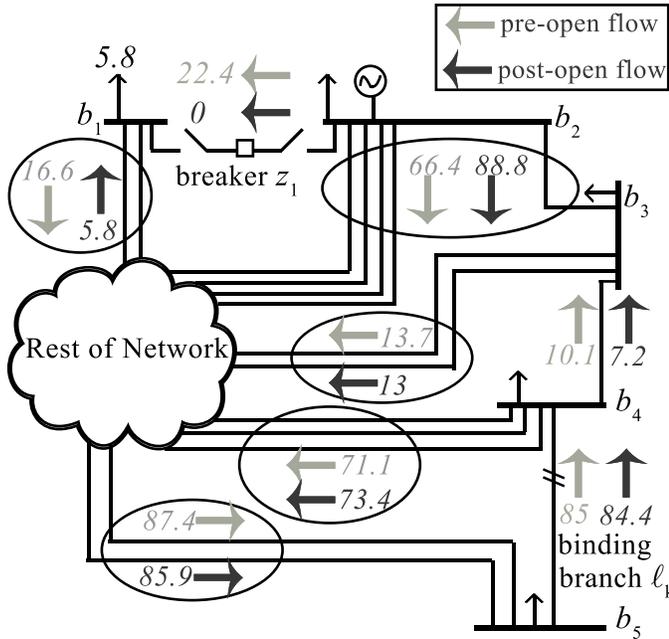
Fig. 6. Flows before and after opening breaker z_1, without redispatch

22.4 MW that flowed across the breaker is routed through the rest of the network. Part of this flow provides counterflow on the branch between busbars b_3 and b_4 and on branch ℓ_k. In general terms, in the post-open network some of the power to meet demand at b_1 is routed to the left of branch ℓ_k as opposed to along the $b_5-b_4-b_3-b_2-b_1$ path in the pre-open network. We note that in this example, there is no single branch that could be opened to produce the same result.

For the one week simulation, Fig. 7 compares the number of breakers opened/kept open by the BOIF/BCT formulations respectively. The two formulations are fully equivalent with the same switchable set being used as detailed in the previous section and are solved to optimality. However, the number of breakers open in the hourly topologies are different between the BCT and BOIF formulations, indicating that there are multiple optimal topologies in the test system considered. The BCT formulation keeps between 0 and 9 breakers in service with an average of about 4 per hour (opens between 30 and 39) while the BOIF formulation keeps between 28 and 38 breakers in service with an average of about 34 per hour (opens between 1 and 11). Note the clear daily
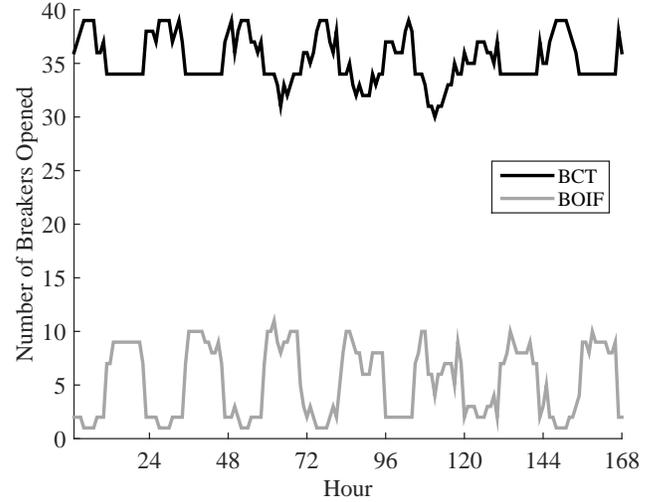

Fig. 7. Breakers kept open in the breaker closing transaction (BCT) formulation and breakers opened in the breaker opening incremental flow (BOIF) formulation.

cycle. Early in the morning there is little congestion so there is little need to change the starting topology. Thus, the BCT formulation closes few, if any, breakers, and the BOIF formulation opens few breakers. Later in the day, during the afternoon hours, congestion increases and both formulations respond by making more changes to their starting topologies: the BOIF formulation opens more breakers and the BCT formulation closes more breakers. Note that with an increased number of switching operations it is possible that constraints not represented by the shift factor models, for example, voltage magnitude, could become violated. In an operational setting, AC validation would have to be performed iteratively with substation reconfiguration (similar to contingency analysis).

To better compare the number of breakers operated in the two models, Fig. 8 shows the number of breakers closed in the BCT model. In most hours the BCT model operates fewer
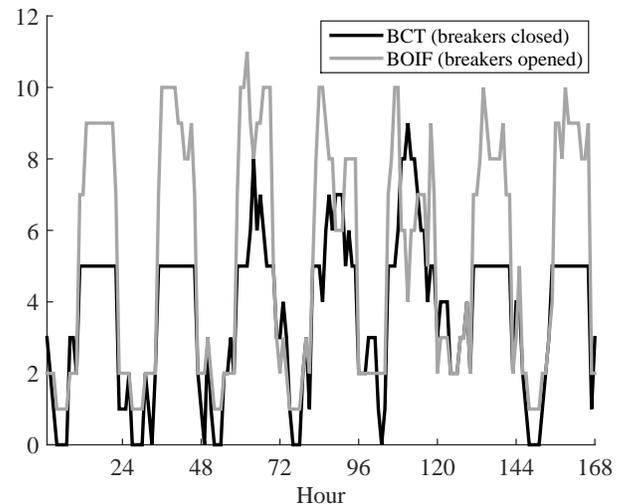

Fig. 8. Number of breakers operated in the BCT and BOIF models

breakers, which is further summarized in Table I. These results are, of course, conditional on the level of congestion in the network. Given the fairly light congestion level[7], in many off-peak hours having a large number of candidate breakers open is an optimal solution. If system conditions were more strained, having most of the candidate breakers open would cause violations in many more hours requiring additional breaker closings under the BCT model. However, these results demonstrate that under light congestion and when a set of breakers is already open, the BCT model may be preferable to the BOIF one in terms of the number of topology changes.

Fig. 9 and Table II compare solution times for the two formulations. While both formulations solve quickly, the BCT
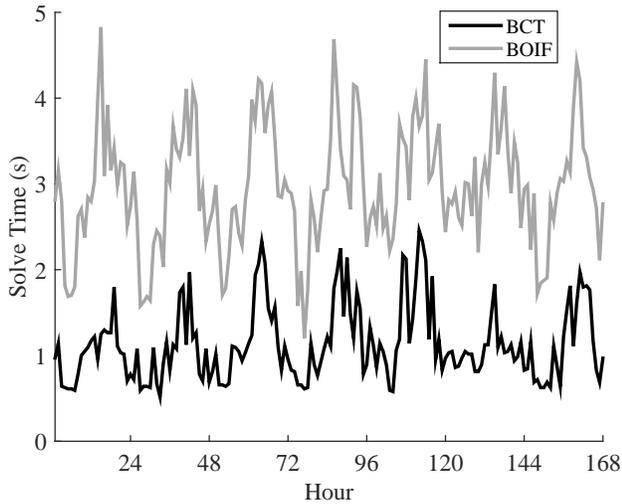

Fig. 9. Solve times, reported in seconds, for the BCT and BOIF formulations

model solves faster on average, especially in off-peak hours. From Figures 8 and 9 we see, as expected, a general correlation between the number of topology changes and the solve time. This further enforces the claim that under certain system conditions, such as with a high number of opened breakers and low load levels, the BCT model may be the appropriate formulation to use.

TABLE I
TOPOLOGY CONTROL ACTIONS IN THE BCT, BOIF, FCT AND JOINT BOIF+FCT FORMULATIONS

| | BCT (closings) | BOIF | FCT | BOIF+FCT | | |
				breakers	branches	total
Min	0	1	1	0	0	1
Max	9	11	4	4	3	6
Median	5	5.5	2	1	2	2
Avg	3.67	5.25	2.14	0.75	1.39	2.14

Next, we consider the joint FCT and BOIF formulation and compare it to the individual FCT and BOIF formulations. Because the production cost savings for the BCT and BOIF model are identical given the same switchable set, we only consider the joint BOIF+FCT model here; the BCT+FCT

[7] The light level of congestion was not specifically chosen and is a characteristic of the available breaker node model for the PJM subarea.

formulation would yield the same savings as the BOIF+FCT formulation. Table I compares the solutions across all formulations. We observe that the joint BOIF+FCT formulation and FCT formulations tend to perform the same number of topology changes. One reason for this is the limited congestion in the system. However, Table I shows that in many hours a breaker opening can serve as a substitute for a branch opening, which can give system operators multiple options for handling certain congestion or contingency events.

TABLE II
BOIF AND BCT SOLVE TIMES (SECONDS)

	BCT	BOIF
Min	0.52	1.20
Max	2.45	4.83
Avg	1.13	2.96

Fig. 10 shows the cost of congestion savings for the three models. Compared to the FCT or BOIF formulation, the joint BOIF+FCT formulation achieves greater cost of congestion savings. The same relationship, although less pronounced, is
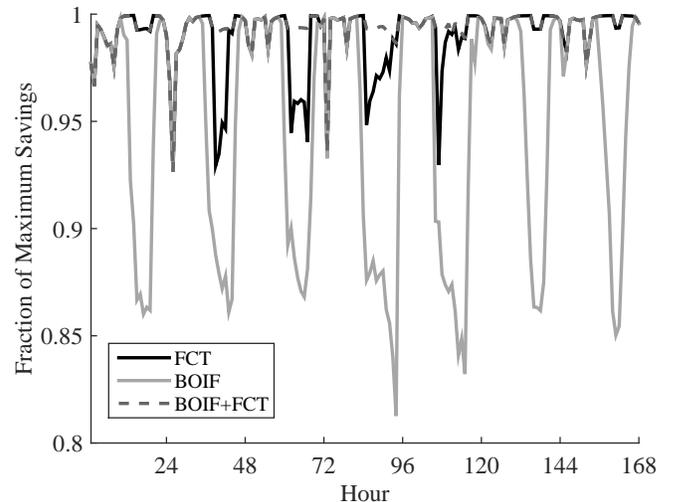

Fig. 10. Relative Cost of Congestion Savings as a fraction of the cost of congestion under the full topology for the BOIF, FCT and joint formulations

observed in terms of production cost savings with the BOIF, FCT and joint formulations averaging 29.4%, 31.3% and 31.5% respectively. Since we are modeling a small number of contingency constraints and system conditions are light, all of the formulations are able to almost entirely relieve network congestion during off-peak hours. During certain peak hours, the joint BOIF+FCT formulation outperforms the FCT formulation and significantly outperforms the BOIF formulation. Due to the naive approach taken to select candidate breakers, this result is not very surprising. Fig. 10 re-affirms the intuition that having the ability to reconfigure substations in addition to switching branches can improve system operations (as measured by cost savings, increased overload relief, etc.).

Note that the above results include a small number of contingency constraints that were binding under historical conditions. Including additional contingency constraints would

further reduce the switchable set under the BCT formulation due to islanding, leading to fewer degrees of freedom, and consequently less savings. While initially restricting the switchable set in the BCT formulation guarantees that the final topology is feasible with respect to contingency constraints, each candidate set of breakers must be tested for islands under every contingency, which can become time consuming. Having more degrees of freedom, in terms of selecting switchable breakers, would give system operators additional flexibility to select an optimal subset of breakers to switch (only a few would typically be switched). The BOIF formulation specifically addresses this issue by starting with a topology where candidate breakers are closed. Since this starting topology is feasible, all switchable breakers can be considered for switching and the constraint set will prevent islanding. Even with four contingency constraints, we restricted the switchable set from 57 to 39 breakers to ensure that the base BCT topology is feasible. Although for the test system simulated, including the additional 18 breakers does not contribute to congestion cost savings given the light system conditions.

VII. DATA AND CALCULATION REQUIREMENTS FOR A LARGE SYSTEM

To provide a practical example around the numerical experiments in the previous section, we evaluate the additional data storage and matrix calculations required by the BCT and BOIF formulations for a large system of a size similar to PJM. The bus-branch representation of the PJM network has the following approximate dimensions:

- 15,000 buses
- 4,000 monitored branches
- 6,000 single and multi-element contingencies

Usually the number of constraints included in any optimization problem is significantly smaller than what is shown above, especially for contingency constraints, many of which are checked through contingency analysis. To better reflect this reduction we assume that a total of 100 constraints, each monitoring the flow of one branch under one contingency are included in the optimization problem (with all contingencies being unique). We further assume that 50 bus-splitting breakers are to be considered in both formulations.

For the BCT formulation we need to store the nodal susceptance matrices corresponding to nodes associated with breakers for each contingent topology. Given the model dimensions above, we first calculate $100 \times 15,000 \times 15,000 = 2.25 \times 10^{10}$ additional values. For each contingent topology we then store a submatrix of dimension 100×100 (we assumed 50 breakers) resulting in a final nodal susceptance matrix of size

$$|\mathbf{B}^{-1}| = 100 \times 100 \times 100 = 1.0 \times 10^6 \qquad (61)$$

In contrast, the BOIF formulation requires calculating a vector of PTDFs ratios (for each monitored branch with respect to a breaker's reference branch) for each breaker and contingent topology. For the large system of interest this means an additional data size of

$$|\mathbf{\Gamma}| = 100 \times 50 \times 100 = 5.0 \times 10^5 \qquad (62)$$

Calculating each column of matrix $\mathbf{\Gamma}$ requires computing an auxiliary PTDF matrix, which is approximately the same amount of work as calculating auxiliary shift factor matrices. For the large system, this means an additional $100 \times 50 = 50,000$ shift factor matrices, each of dimension $100 \times 15,000 = 1.5 \times 10^6$ for a total of 7.5×10^{10} values. Once the auxiliary PTDF matrices are calculated, only the columns corresponding to cutsets are stored (reflected by the dimension of $\mathbf{\Gamma}$). The base topology shift factor matrix for the BCT formulation is also larger than in the BOIF formulation since all candidate breakers are open and each busbar is explicitly represented. In contrast, the base topology in the BOIF formulation is consolidated, resulting in 50 fewer columns across 100 contingencies.

For the large system considered, the BOIF formulation requires an additional order of magnitude in storage but the same order of magnitude in additional calculations. From (61) we observe that as the number of breakers grows, the storage requirements for the BCT formulation grow quadratically in the number of breakers, however, the number of additional calculations remain invariant (the nodal susceptance matrix is calculated for all nodes). In the BOIF formulation, the storage requirements grow linearly in the number of breakers, (62), however, number of addition calculations grows by the product of the number of monitored branches and nodes (each breaker requires an auxiliary shift factor matrix). Thus, the BOIF formulation requires less data to be stored at the expense of additional auxiliary calculations.

VIII. CONCLUDING REMARKS

This paper derives a shift factor framework for modeling breakers that connect busbars within a substation and presents two MIP formulations to optimize substation configuration in the SCOPF problem. The BCT-based formulation starts with a topology where candidate breakers are disconnected and the remaining substation zero-impedance networks are collapsed into their equivalent buses. This results in a compact model since we collapse a large part of the network but requires that the opening of all candidate breakers does not island the system under any contingency. The second, BOIF-based formulation starts with a fully closed network and the model decides on candidate breakers to disconnect. The BOIF formulation provides more freedom to choose candidate branches, at the expense of additional calculations and memory requirements – for each breaker we have to pre-calculate a vector of PTDF ratios (40).

Computationally, the two formulations perform similarly given the same switchable set of breakers. For the test system simulated we observe that the BCT model solves faster and typically opens fewer breakers. While we do not expect this result to hold with additional contingency constraints or under tighter system conditions, we see that despite the non-islanding restrictions, the BCT model can be the better choice for some applications that start with several breakers open and look for the optimal re-closings. For other applications that require identification of breakers to open among a broad set or to select among possible reconfigurations of a substation, the

BOIF formulation is the more appropriate choice. It does not place non-islanding restrictions on the entire switchable set, and therefore allows for a more extensive switchable set.

Given the low congestion conditions and the relative cost savings achieved in most hours through switching actions, the additional breakers the BOIF formulation can optimize over would not provide additional benefits in the test system considered. However, in general we expect the BOIF model to generate more savings than the BCT model. With additional contingency constraints, for example, the non-islanding condition imposed on the candidate set of breakers by the BCT formulation would significantly limit the switchable set. As the number of contingency constraints increases (PJM models approximately 6,000 contingencies in its contingency analysis process) jointly opening all candidate breakers will likely cause islands. Further, selecting a candidate set of breakers under the BCT formulation requires testing each set for islands under every contingency, which quickly becomes computationally expensive.

In the simulations reported in this paper, only breakers that split a bus were considered as switchable. This is generally consistent with the type of breakers operated by PJM. However, being able to identify promising candidate breakers using policies such as the line profit that exist for branch selection would be very useful in the context of the shift factor formulation. This topic has not been widely studied and is a subject of future research in this area.

APPENDIX

Proof that breaker opening incremental flow ratios are well defined

We wish to prove that the ratio below, representing changes in flow due to the opening of a breaker, does not depend on the susceptance of that breaker.

$$\frac{\Delta f_\ell^z}{\Delta f_k^z} \quad (63)$$

To show that the ratio above is in fact well defined we first simplify the ratio and expand it in terms of the nodal susceptance matrix

$$\frac{\Delta f_\ell^z}{\Delta f_k^z} = \frac{LODF_\ell^z}{LODF_k^z} = \frac{\phi_\ell^z}{\phi_k^z} =$$
$$\frac{\tilde{b}_\ell(B_{m,i}^{-1} - B_{i,i}^{-1} - B_{m,j}^{-1} + B_{i,j}^{-1})}{\tilde{b}_k(B_{n,i}^{-1} - B_{i,i}^{-1} - B_{n,j}^{-1} + B_{i,j}^{-1})} \quad (64)$$

Next, we express the nodal susceptance matrix in the following block form to explicitly confine all terms containing the susceptance, $\tilde{b}_z$, of the breaker to a small submatrix:

$$\mathbf{B} = \left[\begin{array}{cc} \hat{\mathbf{B}} & \mathbf{b} \\ \mathbf{b}' & \mathbf{C} \end{array} \right] \quad (65)$$

$\hat{\mathbf{B}}$ represents the nodal susceptance matrix with rows and columns i, j removed, $\mathbf{b}$ corresponds to columns i, j in the nodal susceptance matrix and $\mathbf{C}$ is a 2x2 sub-matrix corresponding to rows and columns i, j. Given the structure of the nodal susceptance matrix,[8]

$$(\mathbf{B})_{ii} = \sum_{\ell \in i} \tilde{b}_\ell \quad (66)$$

$$(\mathbf{B})_{ij} = \mathbf{1}_{(\ell=(i,j))}(-\tilde{b}_\ell) \quad (67)$$

$\mathbf{C}$ can be expressed as

$$\mathbf{C} = \left[\begin{array}{cc} \tilde{b}_z + c & -\tilde{b}_z \\ -\tilde{b}_z & \tilde{b}_z + d \end{array} \right] \quad (68)$$

where c and d are some values that do not depend on $\tilde{b}_z$. We now apply Woodbury's matrix inversion lemma to get an explicit value for the ratio of PTDFs. Note that all the values required in (64) are in the sub-matrices $\mathbf{b}$ and $\mathbf{C}$. The inverse of both of these blocks are

$$\left[\begin{array}{cc} ... & -\hat{\mathbf{B}}^{-1}\mathbf{b}(\mathbf{C} - \mathbf{b}'\hat{\mathbf{B}}^{-1}\mathbf{b})^{-1} \\ ... & (\mathbf{C} - \mathbf{b}'\hat{\mathbf{B}}^{-1}\mathbf{b})^{-1} \end{array} \right] \quad (69)$$

and require the inverse of $(\mathbf{C} - \mathbf{b}'\hat{\mathbf{B}}^{-1}\mathbf{b})$, which has a form similar to (68).

$$(\mathbf{C} - \mathbf{b}'\hat{\mathbf{B}}^{-1}\mathbf{b}) = \left[\begin{array}{cc} \tilde{b}_z + g & -\tilde{b}_z - e \\ -\tilde{b}_z - e & \tilde{b}_z + h \end{array} \right] \quad (70)$$

Since this is a 2x2 matrix we can express the inverse as

$$(\mathbf{C} - \mathbf{b}'\hat{\mathbf{B}}^{-1}\mathbf{b})^{-1} = \frac{1}{det} \left[\begin{array}{cc} \tilde{b}_z + h & \tilde{b}_z + e \\ \tilde{b}_z + e & \tilde{b}_z + g \end{array} \right] \quad (71)$$

Where the determinant is given by

$$det = \tilde{b}_z(g + h - 2e) + gh - e^2 \quad (72)$$

Using (71) we can now express the terms in (64). We expand only the numerator in (73), the denominator has the same structure. The subscripts m, n refer to the row index.

$$\Delta f_\ell^z = \tilde{b}_\ell \Big(-\frac{1}{det}\hat{\mathbf{B}}_m^{-1}\mathbf{b} \left[\begin{array}{c} b_z + h \\ b_z + e \end{array} \right] - \frac{1}{det}(b_z + h)$$
$$+ \frac{1}{det}\hat{\mathbf{B}}_m^{-1}\mathbf{b} \left[\begin{array}{c} b_z + e \\ b_z + g \end{array} \right] + \frac{1}{det}(b_z + e) \Big) \quad (73)$$

All terms are multiplied by $\frac{1}{det}$, which cancel with the same term in the denominator. Further, all terms that multiply b_z in (73) cancel out and we are left with an expression that no longer depends on the susceptance of the breaker.

$$\frac{\Delta f_\ell^z}{\Delta f_k^z} = \frac{\tilde{b}_\ell\Big(\hat{\mathbf{B}}_m^{-1}\mathbf{b} \left[\begin{array}{c} h + e \\ e + g \end{array} \right] + h - e\Big)}{\tilde{b}_k\Big(\hat{\mathbf{B}}_n^{-1}\mathbf{b} \left[\begin{array}{c} h + e \\ e + g \end{array} \right] + h - e\Big)} \quad (74)$$

While explicitly calculating the above expression for every breaker is impractical, we do not need to do so. By replacing the infinite susceptance of the breaker with an arbitrary finite number, we can calculate an additional PTDF matrix and use it to find the ratios in (64).

---

[8]The notation $\ell \in i$ means all branches ℓ that are incident to node i. The indicator function $\mathbf{1}_{(\ell=(i,j))}$ is 1 when branch ℓ connects nodes i and j.

References

[1] A. Mazi, B. Wollenberg, and M. Hesse, "Corrective control of power system flows by line and bus-bar switching," *IEEE Trans. Power Syst.*, vol. 1, no. 3, pp. 258–264, Aug. 1986.

[2] A. G. Bakirtzis and A. P. S. Meliopoulos, "Incorporation of switching operations in power system corrective control computations," *IEEE Trans. Power Syst.*, vol. 2, no. 3, pp. 669–675, Aug. 1987.

[3] W. Shao and V. Vittal, "Corrective switching algorithm for relieving overloads and voltage violations," *IEEE Trans. Power Syst.*, vol. 20, no. 4, pp. 1877–1885, Nov. 2005.

[4] G. Schnyder and H. Glavitsch, "Security enhancement using an optimal switching power flow," *IEEE Trans. Power Syst.*, vol. 5, no. 2, pp. 674–681, May 1990.

[5] H. Glavitsh, "Power system security enhanced by post-contingency switching and rescheduling," in *Proc. IEEE Power Tech 1993*, Sep. 1993, pp. 16–21.

[6] R. Bacher and H. Glavitsch, "Loss reduction by network switching," *IEEE Trans. Power Syst.*, vol. 3, no. 2, pp. 447–454, May 1988.

[7] S. Fliscounakis, F. Zaoui, G. Simeant, and R. Gonzalez, "Topology influence on loss reduction as a mixed integer linear programming problem," in *Proc. IEEE Power Tech 2007*, Jul. 2007, pp. 1987–1990.

[8] R. O'Neill, R. Baldick, U. Helman, M. Rothkopf, and W. Stewart, "Dispatchable transmission in RTO markets," *IEEE Trans. Power Syst.*, vol. 20, no. 1, pp. 171–179, Feb. 2005.

[9] E. B. Fisher, R. P. O'Neill, and M. C. Ferris, "Optimal transmission switching," *IEEE Trans. Power Syst.*, vol. 23, no. 3, pp. 1346–1355, Aug. 2008.

[10] K. W. Hedman, M. C. Ferris, R. P. O'Neill, E. B. Fisher, and S. S. Oren, "Co-optimization of generation unit commitment and transmission switching with n-1 reliability," *IEEE Trans. Power Syst.*, vol. 25, no. 2, pp. 1052–1063, May 2010.

[11] C. Liu, J. Wang, and J. Ostrowski, "Static security in multi-period transmission switching," *IEEE Trans. Power Syst.*, vol. 27, no. 4, pp. 1850–1858, 2012.

[12] E. Goldis, X. Li, M. C. Caramanis, B. Keshavamurthy, M. Patel, A. Rudkevich, and P. A. Ruiz, "Applicability of topology control algorithms (TCA) to a real-size power system," in *Proc. 51st Allerton Conference on Communication, Control, and Computing*, Monticello, IL, Oct 2013, pp. 1349–1352.

[13] P. A. Ruiz, J. M. Foster, A. Rudkevich, and M. C. Caramanis, "Tractable transmission topology control using sensitivity analysis," *IEEE Trans. Power Syst.*, vol. 27, no. 3, pp. 1550–1559, Aug. 2012.

[14] P. A. Ruiz, A. M. Rudkevich, M. C. Caramanis, E. A. Goldis, E. Ntakou, and C. R. Philbrick, "Reduced MIP formulation for transmission topology control," in *Proc. 50th Allerton Conf. on Communications, Control and Computing*, Monticello, IL, Oct. 2012, pp. 1073–1079.

[15] E. Goldis, M. C. Caramanis, C. R. Philbrick, A. Rudkevich, and P. A. Ruiz, "Security-constrained MIP formulation of topology control using loss-adjusted shift factors." in *Proc. 47th Hawaii International Conference on System Science*, Jan 2014, pp. 2503–2509.

[16] F. Zaoui, S. Fliscounakis, and R. Gonzalez, "Coupling OPF and topology optimization," in *Proc. 15th Power System Computation Conference'*, Liége, Belgium, Aug 2005.

[17] W. Shao and V. Vittal, "BIP-Based OPF for line and bus-bar switching to relieve overloads and voltage violations," in *Proc. Power Systems Conference and Exposition*, Atlanta, GA, Oct 2006.

[18] H. Glavitsch, "Switching as means of control in the power system," *International Journal of Electrical Power and Energy Systems*, vol. 7, no. 2, pp. 92–100, Apr 1985.

[19] M. Heidarifar, M. Doostizadeh, and H. Ghasemi, "Optimal transmission reconfiguration through line switching and bus splitting," in *Proc. IEEE PES General Meeting*, July 2014, pp. 1–5.

[20] M. Heidarifar and H. Ghasemi, "A network topology optimization model based on substation and node-breaker modeling," *IEEE Transactions on Power Systems*, vol. 31, no. 1, pp. 247–255, Jan 2016.

[21] E. Lourenço, N. da Silva, and A. Costa, "Fast decoupled steady-state solution for power networks modeled at the bus section level," in *Proc. 2009 IEEE PowerTech*, Bucharest, Hungary, June 2009, pp. 1–7.

[22] I. Vágó, *Graph Theory: Application to the Calculation of Electrical Networks*, ser. Studies in electrical and electronic engineering. Elsevier, 1985, pp. 31–32, 46–48.

[23] J. Gentle, *Matrix Algebra: Theory, Computations, and Applications in Statistics*. Springer, 2007, ch. 3, p. 89.

[24] D. Fuller, "A fast heuristic for optimal transmission switching." Austin, TX: Presented at *INFORMS Annual Meeting*, Nov 2010.

[25] B. Kocuk, H. Jeon, S. S. Dey, J. Linderoth, J. Luedtke, and X. A. Sun, "A Cycle-Based Formulation and Valid Inequalities for DC Power Transmission Problems with Switching," *Accepted for publication in Operations Research (2016).*

Evgeniy Goldis (S'12) received his B.S. from Harvey Mudd College in 2004 and his M.A. (2007) and Ph.D. (2015) from Boston University. His research interests include electricity and natural gas market design and optimization, as well as high-performance and cloud computing. He is currently the Chief Technology Officer of Newton Energy Group (NEG) and a senior consultant with TCR.

Pablo A. Ruiz (S'05, M'09) received the degree of Ingeniero Electricista (2002) from Universidad Tecnolgica Nacional-Santa Fe, Argentina, and the M.Sc. (2005) and Ph.D. (2008) degrees from the University of Illinois at Urbana-Champaign. He is Research Associate Professor of Mechanical Engineering at Boston University, Senior Associate in the Utilities Practice Area at The Brattle Group and Co-Founder, President and Chief Technology Officer at NewGrid, Inc. He was previously with AREVA T&D and Charles River Associates. His research is in power and gas systems and markets, including optimization, computations, economics, operations, and planning.

Michael C. Caramanis (M'79) received his B.S. (1971) degree from Stanford University and his M.S. (1972) and Ph.D. (1976) from Harvard University. He is a Boston University Professor of Mechanical and Systems Engineering. Prof. Caramanis chaired the Greek Regulatory Authority for Energy and the International Energy Charters Investment Group (20014-2008), was personally involved in power market implementations in England (1989-90) and Italy (2000-03), and his written work has influenced Power Market design in the US and Europe. His current application domain focus is marginal costing and dynamic pricing on smart power grids, grid topology control for congestion mitigation, and the extension of power markets to include distribution connected loads, generation, and resources. He is coauthor of Spot Pricing of Electricity, Kluwer, 1987, and more than 100 refereed publications. His disciplinary background is in Mathematical Economics, Optimization, and Stochastic Dynamic Decision Making.

Xiaoguang Li received his B.A.Sc. and M.A.Sc. degrees in electrical engineering from the University of Toronto, Toronto, ON, Canada in 2009 and 2011, respectively. He is Co-Founder and Director of NewGrid, Inc., and a Consultant with The Brattle Group, Cambridge, MA. He was previously with Boston University and Charles River Associates. His research focus is on decision support software for power systems and electricity markets.

C. Russ Philbrick (M'99, SM'09) received his B.S. from Duke University in 1983 and his M.S. (1994) and Ph.D. (1997) from Stanford University. Through Polaris Systems Optimization, he develops tools to support power-grid reliability, efficiency and integration of renewable energy. Prior roles include Principle Power Systems Engineer (ALSTOM Grid 1999 to 2010), Associate Professor (Washington State University and Albrook Hydraulics Lab 1997 to 1999) and Submarine Officer (U.S. Navy 1984 to 2012). His experience includes nuclear plant operations and industrial engineering, and fields of interest include operations research, business process analysis, economics, probabilistic methods, and optimization. He has developed security-constrained unit commitment and economic dispatch tools broadly used by power markets and utilities.

Aleksandr Rudkevich (M'09) received his M.Sc (1978). from the Gubkin Russian State University of Oil and Gas, Moscow, Russia and his Ph.D. (1988) from the Melentiev Energy Systems Institute of the Russian Academy of Sciences, Irkutsk, Russia. He is President and Co-Founder of Newton Energy Group with over 30 years of experience in energy economics, regulatory policy, and quantitative analyses of market fundamentals for electric power, natural gas and crude oil production and supply. His specialties include complex modeling of energy systems with applications to energy asset valuation, price forecasting, regulatory policy and market design.